COMPUTATIONAL BIOLOGY

Linear Motif Atlas for Phosphorylation-Dependent Signaling

Martin Lee Miller,[1,2*] Lars Juhl Jensen,[2,3*] Francesca Diella,[3] Claus Jørgensen,[4] Michele Tinti,[5] Lei Li,[6] Marilyn Hsiung,[4] Sirlester A. Parker,[7] Jennifer Bordeaux,[7] Thomas Sicheritz-Ponten,[1] Marina Olhovsky,[4] Adrian Pasculescu,[4] Jes Alexander,[8] Stefan Knapp,[9] Nikolaj Blom,[1] Peer Bork,[2,10] Shawn Li,[6] Gianni Cesareni,[5] Tony Pawson,[4] Benjamin E. Turk,[7] Michael B. Yaffe,[8†] Søren Brunak,[1,2†] Rune Linding[4,8,11†]

(Published 2 September 2008)

Systematic and quantitative analysis of protein phosphorylation is revealing dynamic regulatory networks underlying cellular responses to environmental cues. However, matching these sites to the kinases that phosphorylate them and the phosphorylation-dependent binding domains that may subsequently bind to them remains a challenge. NetPhorest is an atlas of consensus sequence motifs that covers 179 kinases and 104 phosphorylation-dependent binding domains [Src homology 2 (SH2), phosphotyrosine binding (PTB), BRCA1 C-terminal (BRCT), WW, and 14–3–3]. The atlas reveals new aspects of signaling systems, including the observation that tyrosine kinases mutated in cancer have lower specificity than their non-oncogenic relatives. The resource is maintained by an automated pipeline, which uses phylogenetic trees to structure the currently available in vivo and in vitro data to derive probabilistic sequence models of linear motifs. The atlas is available as a community resource (http://netphorest.info).

INTRODUCTION

Proteins in eukaryotes consist of two fundamentally different types of functional building blocks or modules: protein domains and linear motifs. Whereas domains are often defined as large (>30 residues) globular units with defined binding or catalytic activities (*1*–*4*), linear motifs are short colinear sequences, typically of less than 10 residues, that often reside in disordered regions (*1*). Domains are frequently conserved over long evolutionary distances and change through divergent evolution (*2*, *3*), whereas linear motifs evolve much more rapidly (*5*) and can likely arise through convergent evolution because of their short length (*6*).

Posttranslational modification of linear motifs is a driving force behind directional and dynamic protein-interaction networks (*7*). One such modification is phosphorylation, which modulates the binding of protein domains (such as SH2 and BRCT) and thereby creates logic gates (*7*). This enables the cell to swiftly integrate and respond to combinations of internal and external cues. Advances in mass-spectrometry techniques have led to the identification of thousands of in vivo phosphorylation sites (*8*–*11*). However, most of these sites are uncharacterized with respect to their roles in signaling, because the kinases responsible for their phosphorylation and the proteins that recognize these phosphorylated sites are often unknown (*12*). Linking these sites to the hundreds of protein kinase catalytic domains (from hereon referred to as kinases) and modular binding domains is a challenge for in-depth understanding of cellular signaling processes.

Whereas several resources exist for identifying protein domains from sequence alone, for example, SMART (*3*) and Pfam (*2*), equally powerful resources do not exist for linear motifs primarily because of their low information content (*4*, *13*, *14*). Numerous methods have been developed to predict potential phosphorylation sites for specific kinases; these include the pioneering work (Scansite) on position-specific scoring matrices (PSSMs) derived from peptide libraries (*13*, *15*–*17*), manually constructed sequence patterns (*14*, *18*, *19*), and a variety of machine-learning algorithms that have been trained on in vivo phosphorylation data (*20*–*24*). As new, powerful phosphoproteomics methods continue to increase our knowledge of cellular phosphorylation sites (*8*–*11*), models that are optimized to classify experimentally identified sites (rather than to predict them) according to the relevant kinase family or corresponding binding domains are increasingly important. Classification is a difficult task, because of the limited number of known targets for individual kinases and phosphorylation-dependent binding domains (phospho-binding domains) and the large number of different domains [for example, ~518 kinases in human (*25*)], many of which recognize similar sequence motifs.

Here, we present NetPhorest, an atlas of linear motifs involved in phosphorylation-dependent signaling, which consists of 125 sequence models that classify the substrates and ligands of 179 protein kinases and 104 phospho-binding domains (phosphotyrosine: SH2 and PTB; phosphoserine and phosphothreonine: 14-3-3, BRCT, and WW). We also describe the computational framework and pipeline used for automatically constructing this resource on the basis of currently available data and experiments performed as part of this study. NetPhorest can thus be

[1]Center for Biological Sequence Analysis, Technical University of Denmark, 2800 Lyngby, Denmark. [2]The Novo Nordisk Foundation Centre for Protein Research, University of Copenhagen, 2200 Copenhagen, Denmark. [3]European Molecular Biology Laboratory, 69117 Heidelberg, Germany. [4]Samuel Lunenfeld Research Institute, Mount Sinai Hospital, M5G 1X5 Toronto, Ontario, Canada. [5]Uni versity of Rome, Tor Vergata, 00133 Rome, Italy. [6]University of Western Ontario, N6A 5C1 London, Ontario, Canada. [7]Department of Pharmacology, Yale University School of Medicine, New Haven, 06520 CT, USA. [8]Center for Cancer Research, Massachusetts Institute of Technology, Cambridge, 021329 MA, USA. [9]Structural Genomics Consortium, University of Oxford, OX3 7DQ Oxford, UK. [10]Max-Delbrück-Centre for Molecular Medicine, 13092 Berlin, Germany. [11]Cellular & Molecular Logic Team, The Institute of Cancer Research, SW3 6JB London, UK.
*These authors contributed equally to this work.
†To whom correspondence should be addressed. E-mail: brunak@cbs.dtu.dk (S.B.), myaffe@mit.edu (M.B.Y.), and rune.linding@gmail.com (R.L.)

maintained as an up-to-date resource for analysis of phosphorylation-dependent signaling.

RESULTS

The NetPhorest resource accomplishes four major goals. First, it provides the most comprehensive atlas of linear motifs recognized by specific protein kinases and domains that bind to phosphorylated residues. Second, it contains a collection of probabilistic classifiers that enables experimentally identified phosphorylation sites to be classified (according to kinases and phospho-binding domains) with much higher accuracy than existing sequence-based methods. Third, an automatic pipeline keeps the resource up to date with the latest data from in vivo and in vitro experiments. Fourth, the classifiers are made available both through a Web interface (http://netphorest.info) and as a fast, portable stand-alone software application.

Tree-based data organization and redundancy reduction

The first essential steps toward automated construction of sequence models of linear motifs are the collection and organization of the data. We use two fundamentally different types of experimental data. First, decades of targeted studies have resulted in a relatively large and fairly reliable data set of in vivo protein-phosphorylation sites that are linked to at least one kinase [Phospho.ELM (*26*)] or phospho-binding domain [DOMINO (*27*)]. Second, several in vitro methods allow the interrogation of kinase specificity by degenerate peptide libraries (*15*, *17*, *28*). Whereas the latter represent the most abundant data type, for our purposes it is essential to design a framework that can combine the two, resulting in a single classification system. To this end, we map both in vivo and in vitro data onto phylogenetic trees of the kinase and phospho-binding domains (*25*, *29*) (Fig. 1A and fig. S2), which capture how similar the domains are to one another and thereby how likely they are to have similar substrate specificities. The tree-based approach thus enables us to make inferences based on the fact that highly similar domains typically have similar substrate specificities, but it does not assume that dissimilar domains necessarily have dissimilar substrate specificities.

The domain trees also serve as a powerful data structure that enables us to automatically incorporate all data related to any family or subfamily of domains. Thus, the trees are used to automatically compile training and benchmark data sets for specific domains and for families of related domains (Fig. 1B). For example, known in vivo substrates of all protein kinase C (PKC) isoforms would be included as positive examples in the data set for the PKC family, whereas negative examples would be drawn from the known in vivo substrates of all other kinases. By contrast, the data set on PKCα would include only its own substrates as positive examples, and substrates of other PKC isoforms and all other kinases would now be considered negative examples. Consequently, the sequence models are evaluated on their ability to discriminate between substrates of different kinases or targets of distinct binding domains, which is the task at hand when interpreting phosphoproteomics data, rather than on their ability to predict phosphorylation sites (*20*–*24*). The exclusion of nonphosphorylated sites also ensures that the sequence-specificity atlas is not distorted by the numerous sites that are not phosphorylated by any kinase because they are structurally inaccessible to all kinases and hence contain no information about their sequence specificity.

Frequently, corresponding phosphorylation sites from sets of similar proteins have been identified in separate studies. These observations cannot be considered independent observations because of their evolutionary relationship, and therefore we eliminate redundant sites for which either the proteins or the sites themselves are too similar in sequence (Fig. 1C, see Methods for details). Because many machine-learning methods as well as accuracy measures work poorly on highly unbalanced data sets in which the numbers of positive and negative examples differ by orders of magnitude (*30*), we randomly reduce each data set to include only five negative examples per positive example.

Constructing sequence models of linear motifs

Early initiatives for ab initio prediction of linear motifs relied on simple consensus patterns compiled from the literature; for example, the pattern [ST]P..[RK] is commonly used to search for cyclin-dependent kinase (CDK) substrates (*14*, *18*, *19*). Although appealing because of their simplicity, such patterns oversimplify the mechanisms that govern kinase–substrate recognition (*20*, *31*). In particular, they are unable to model correlations between individual residues and their joint contribution to the binding energy. Furthermore, the absence of a scoring scheme implies that predictions cannot be sorted according to their reliability, which makes the approach unsuited for large-scale studies.

To represent the relative affinities with which domains recognize different peptide sequences, we use PSSMs and artificial neural networks (ANNs) (*32*), which mainly differ in that the latter can also capture nonlinear correlations between residues. For the in vitro assays that cannot reveal such correlations (*16*, *33*), we construct PSSMs, whereas we train ANNs on the in vivo and peptide-based in vitro phosphorylation data (*34*). Although many other machine-learning algorithms are available, we chose to use ANNs because they are fast to construct and to execute and have been successfully used for predicting various linear motifs (*20*, *35*, *36*). Moreover, different machine-learning algorithms give similar results when trained on the same data (*36*, *37*), and resources are thus better spent, in our view, on improving the quality of the training data and on automation to rapidly accommodate new data rather than on testing many alternative machine-learning algorithms.

Three data sets are needed to construct an ANN: a training set for optimizing the weights, a test set for selecting the optimal network architecture and training parameters, and an independent validation set for assessing the prediction accuracy. To optimally use the available data, we adopt a fourfold cross-validation scheme in which the final sets of positive and negative examples are randomly partitioned into four equal parts, of which we use two for training, one for testing, and one for validation. All 12 possible permutations of these sets are then used for training and evaluating an ensemble of ANNs (Fig. 1D, see Methods for details). Applying this procedure to the currently available data yielded 151 and 134 ANN predictors for substrates of kinases and targets of phospho-binding domains, respectively.

Integration of heterogeneous models

Sequence models of linear motifs produce scores that are not directly comparable between models for different domains. To enable use of a collection of PSSMs and ANNs for classification of phosphorylation sites, this issue must first be resolved. We therefore designed a scoring scheme in which the raw scores from different models are calibrated through benchmarking against a common reference, namely, our compilation of phosphorylation sites. The benchmarking converts the raw scores into probabilistic scores, which, in contrast to the raw scores or percentile scores, can be directly compared between classifiers.

To construct a calibration curve for each ensemble of ANNs, we calculate the fraction of correct predictions within different score intervals on the validation set and fit these values with a sigmoid function (fig. S4, see Methods for details). In case of PSSMs, we first calculated a scaling factor for each PSSM on the basis of its score distribution on random peptides. Subsequently, we calculate individual calibration curves based on the

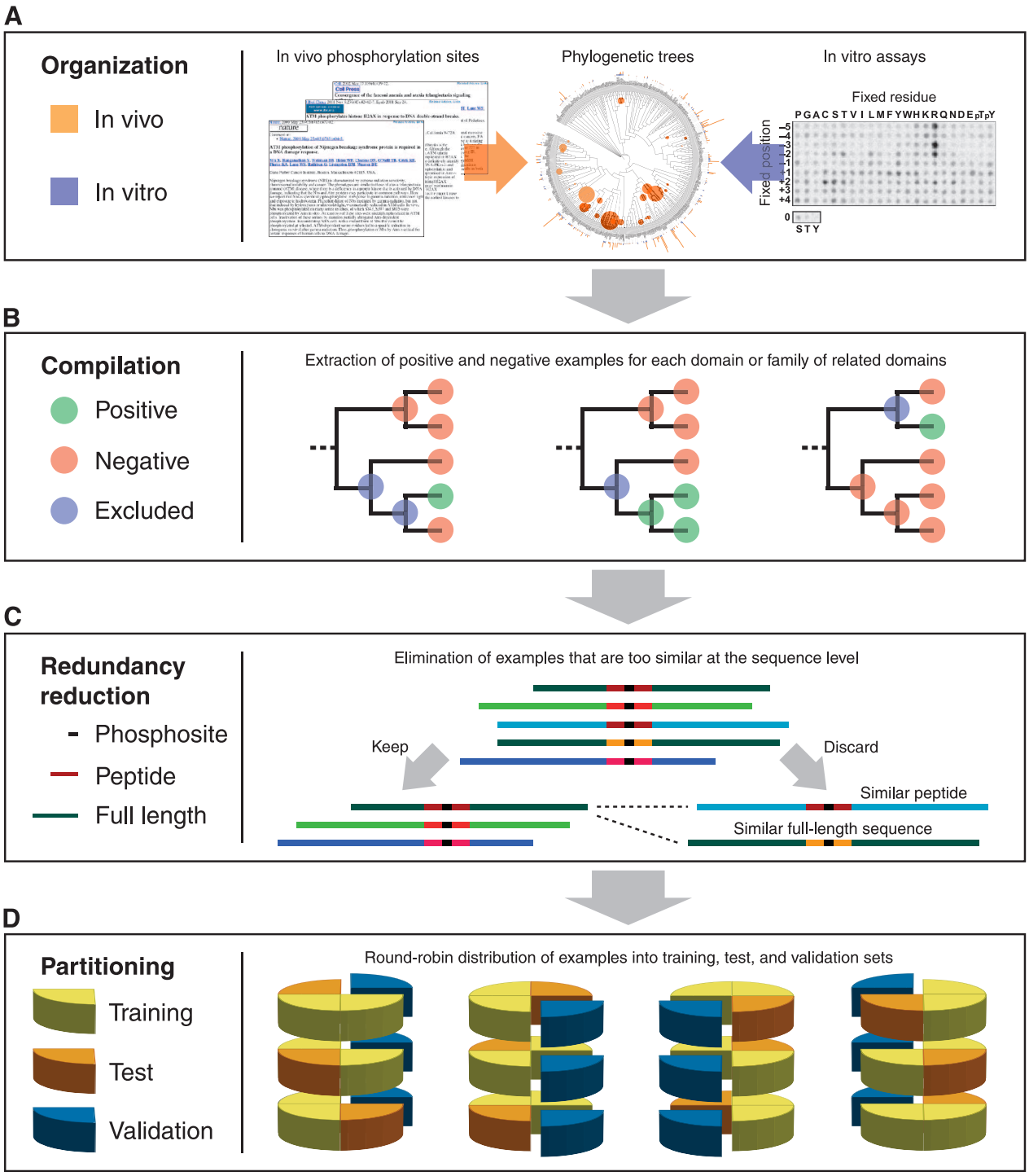

Fig. 1. Tree-based organization, redundancy reduction, and partitioning of data. (A) All available data from in vivo and in vitro experiments for kinase, SH2, and PTB domains are organized by mapping them onto the phylogenetic domain trees. (B) The tree data structure enables us to automatically compile a data set of positive and negative examples for each domain or family of related domains. For a given domain (leafs in the tree) or domain family (branch points in the tree), we exclude phosphorylation sites that cannot be unambiguously designated as positive or negative examples, because they were annotated at a higher level in the tree. (C) Redundant phosphoproteins and phosphorylation sites are identified and eliminated on the basis of sequence similarity of the full-length protein sequence or the phosphorylation sites themselves. (D) Each redundancy-reduced data set is partitioned into four parts that are used for training, test, and validation of ANNs. See fig. S1 for a flowchart of the pipeline, fig. S2 for an overview of the data coverage, and Methods for details.

complete redundancy-reduced data sets when at least 12 sites were known for the kinases or binding domains in question. For the remaining PSSMs, we constructed two generic calibration curves representing the average reliability of PSSMs for kinase and phosphotyrosine-binding domains, respectively.

The resulting calibration curves enable us to estimate the (posterior) probability that a site is recognized by a particular kinase, phospho-binding domain, or family thereof. However, because the fractions of positive examples within the redundancy-reduced data sets do not reflect the corresponding prior probabilities (the probability that a kinase or domain recognizes a site regardless of its sequence), the calibration curves must first be rescaled accordingly. Because the prior probability for each family of kinases or phospho-binding domain is not known, an estimated prior probability was used that is based on the square root of the number of different domains within the family in question; the square root was chosen to take into account that the prior probability increases less than proportionally with size of the family, as similar domains often recognize similar motifs (see Methods for details).

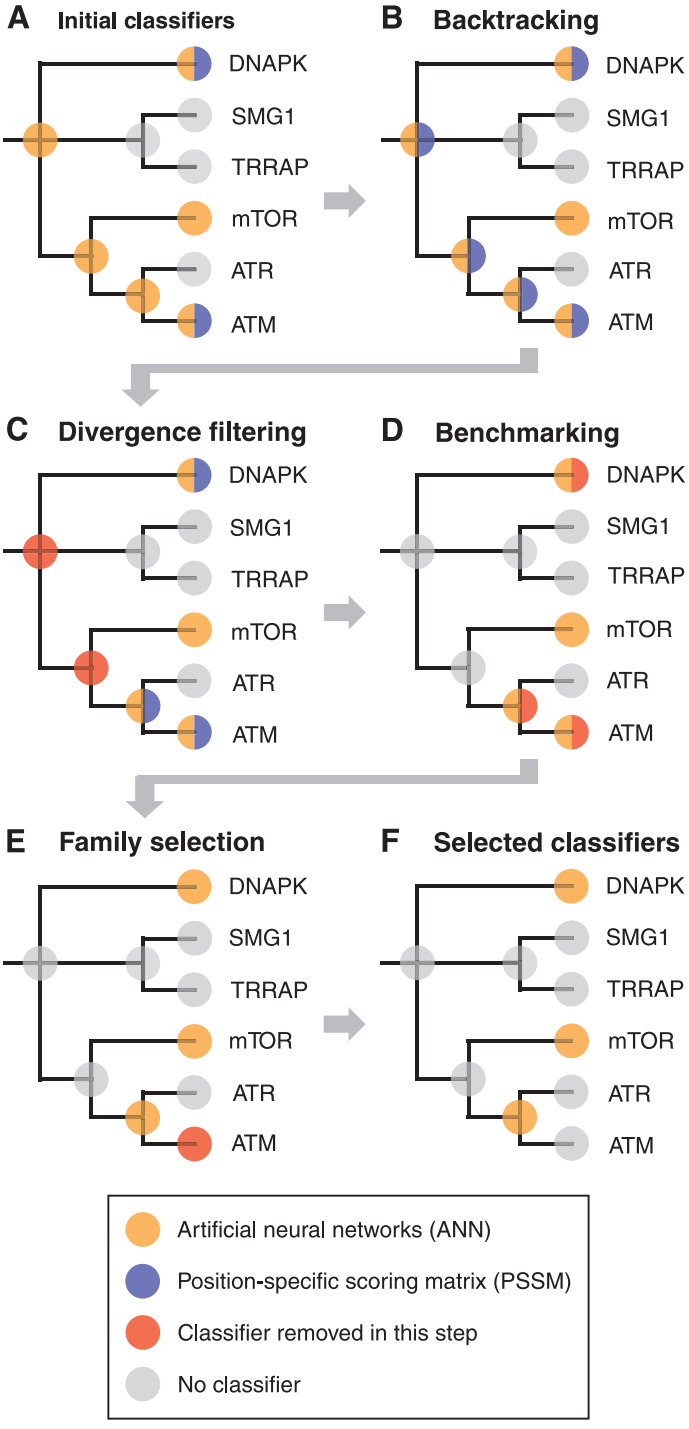

Selecting a nonredundant set of classifiers

The final step in the NetPhorest workflow is to select a set of classifiers that strikes a compromise between having the highest prediction accuracy, the most finely resolved families, and the broadest coverage of kinases and phospho-binding domains. The tree-based organization of the data and the consistent benchmarks of all sequence models are the keys to automating this task (Fig. 2).

First, we assign the classifiers to families of related kinases or phospho-binding domains based on the phylogenetic domain trees. Whereas ANNs naturally belong to the family for which they were trained (Fig. 2A), an in vitro experiment is always performed with a specific purified protein or domain (for example, the ataxia telangiectasia mutated (ATM) protein kinase), yet the resulting PSSM may be better used as a classifier for a family including other closely related domains (for example, the subfamily composed of ATM and ATM Related (ATR), the ATM/ATR subfamily). We thus backtrack each PSSM in the tree and consider it a possible classifier for every node on the path connecting the root of the tree with the node at which the PSSM was initially assigned (Fig. 2B). To avoid assigning a single classifier to an overly divergent family of kinases or phospho-binding domain, we calculate the pairwise sequence similarity of all domain sequences within each family and eliminate families with a self-normalized bit score less than 0.3 (Fig. 2C, see Methods).

Next, we evaluate the predictive performance of the classifiers on the basis of their receiver operating characteristic (ROC) curves, which show sensitivity as function of false-positive rate (fig. S8). We summarize each curve in a single number, the area under the ROC curve (AROC), which is equivalent to the Mann–Whitney *U* statistic (*38*). We discard any of the sequence models that do not perform significantly better than random ($P < 0.05$), as judged by resampling the scores of positive and negative examples to construct a (bootstrapped) AROC distribution (see Methods). In cases where we are still left with several alternative classifiers for the

Fig. 2. Selection of classifiers using the phosphoinositide 3-kinase-related kinase (PIKK) family of kinases as an example. (**A**) ANNs are trained for individual domains, subfamilies, and families of domains; by contrast, the PSSMs are initially assigned to the specific domain with which the in vitro assay was performed. (**B**) As some PSSMs (for example, the one for ATM) may be better used as classifiers for a subfamily of closely related kinases (for example, ATM/ATR), we backtrack all PSSMs toward the root of the tree. (**C**) We eliminate families that contain domains that are highly dissimilar from each other (for example, the PIKK family and the ATM/ATR/mTOR subfamily), in order not to describe highly divergent domains with the same ANNs and PSSMs (see Methods). (**D**) Whenever possible, we benchmark the ANNs and PSSMs and discard classifiers that do not perform significantly better than random expectation. (**E**) A nonredundant set of classifiers is selected that maximizes the average AROC across all kinases, SH2 domains, or PTB domains. (**F**) For the PIKK family of kinases, this procedure selects the ANNs for the ATM/ATR subfamily, mTOR, and DNA-dependent protein kinase (DNAPK) to be the best combination of classifiers. See fig. S3 for an overview of the current selection of classifiers.

same family of domains (for example, an ANN and a Scansite PSSM for the ATM kinase), we select the one with the best predictive performance according to our benchmarks (Fig. 2D).

At this stage we may still have multiple classifiers that cover the same kinase or phospho-binding domain; for example, we may have classifiers for both ATM alone and for the ATM/ATR subfamily (Fig. 2E). To eliminate this redundancy, we select a nonoverlapping set among the remaining classifiers that maximizes the average AROC across all domains. For this purpose, PSSMs that could not be benchmarked because of lack of site-specific data are considered to have the average AROC of PSSMs for the domain type in question (that is, kinase, SH2, PTB, BRCT, WW, or 14–3–3). Any domain that is not covered by a given set of classifiers is considered equivalent to a random predictor (AROC = 0.5). In the case of ATM, this leads to the selection of the ATM/ATR subfamily over ATM alone because the AROC for the subfamily is higher than the average for its two members, ATM and ATR (Fig. 2F). Using these selection criteria, the NetPhorest pipeline yields a nonredundant collection of 125 sequence-based classifiers that cover 179 of 518 kinase domains, 93 of 118 SH2 domains, 8 of 18 phosphotyrosine-binding PTB domains, and the PIN1 WW domain (fig. S3 and table S1). This includes new PSSMs for the kinases LKB1, MST1, TLK1 and TNIK (see Methods). Moreover, NetPhorest currently contains two classifiers for BRCT domains and 14-3-3 proteins, respectively.

Comparison with other methods

Assessing the performance of a computational method is important for two reasons: (i) to quantify the reliability of its predictions on an absolute scale (for example, by calculating posterior probabilities as described above) (Fig. 3, fig. S8, and table S1 for details) and (ii) to determine how it fares relative to existing methods, that is, if scientific progress has been made (*30*). To address the latter issue, we compared NetPhorest to four published methods for kinase-specific prediction of phosphorylation sites [GPS (*22*), KinasePhos (*24*), NetPhosK (*20*), and Scansite (*13*)] and to the simple sequence patterns collected by the ELM (*14*), PROSITE (*19*), and HPRD (*18*) databases.

Because most methods have been trained on data from Phospho.ELM, to make a fair comparison, we benchmarked each method on only the phosphorylation sites that are dissimilar in sequence to those used for developing the NetPhorest method. Provided that at least five positive examples were left, we evaluated the predictive performance of each predictor by calculating the AROC. Using a bootstrap procedure (see Methods), we tested if the AROC of each predictor of each method is significantly ($P < 0.05$) better than random guessing, significantly poorer than the corresponding AROC of NetPhorest, or comparable to it. Of the 140 predictors that could be evaluated, 40 were random, 60 were worse, and 40 had comparable performance to NetPhorest (Fig. 4 and table S2). None of the evaluated predictors were significantly better, this despite the fact that the regular expressions tested may have been derived from some of the examples in our benchmark sets and therefore have an unfair advantage.

We thus conclude that NetPhorest performs significantly better than every other method tested and that more advanced machine-learning methods should be preferred over simple pattern-matching approaches whenever sufficient data exist. This underlines the importance of having a fully automated pipeline that allows new data to be easily incorporated.

Properties of linear motifs

The large number of kinases and phospho-binding domains covered by NetPhorest provides a systematic view of the biochemical features of phosphorylated linear motifs. The average length of a linear motif is often cited as less than 10 amino acids (*13*, *14*). This number agrees well with the average lengths of our automatically selected ANN-based sequence models, which are 11 and 9 amino acids for kinases and phospho-binding domains, respectively. A related issue with linear motifs is the degree to which the positions within a short peptide can be assumed to be independent of each other, that is, how much additional information is present in the inter-residue correlations. To investigate this, we compared the performance of linear and nonlinear ANNs trained on the same data sets, which allowed direct measurement of nonlinearity in the sequence model. Underlining the importance of inter-residue correlations, the average predictive performance (AROC) for kinases drops from 0.79 to 0.75 ($P < 10^{-3}$, Wilcoxon test) when a linear model is used [an ANN with no hidden layer (*32*)]. This is particularly evident for the tyrosine kinases Tec, FLT, CSF1R, and Met, for which the AROC drops by more than 20% when inter-residue correlations are not considered (table S1). This limits the usefulness of in vitro assays that reveal only position-specific amino acid preferences.

Comparing sequence specificities of the many kinases and phosphotyrosine-binding domains revealed that, whereas similar protein kinases and phosphotyrosine-binding domains tend to recognize similar substrates or ligands, the correlation between domain and substrate similarity is far from perfect ($R^2 = 0.18$, $P < 10^{-12}$ and $R^2 = 0.31$, $P < 10^{-6}$ for kinases and SH2 domains, respectively; only domain pairs with a self-normalized bit score of 0.3 or higher are considered) (fig. S5). Whereas closely related domains typically recognize similar sequence motifs, the reverse is not true because even distinct domain families that diverged before the last common ancestor of eukaryotes may have similar sequence specificities. Prominent examples of the latter include the proline-directed kinases [CDKs and the mitogen-activated protein kinases (MAPKs)] and the kinases ATM, ATR, and DNAPK that recognize a glutamine (Q) in position +1 relative to the phosphorylated serine or threonine residue (fig. S5). However, we observe subtle differences in sequence specificity even among the proline-directed kinases. Whereas CDK1, 2, 3, and 5 all show the canonical preference for positively charged residues in position +3 (and to a lesser extent, +2 and +4), the MAPKs favor proline or leucine in position −2 [as well as −1 in case of the c-Jun N-terminal kinase (JNK) subfamily] (fig. S7).

DISCUSSION

The objective, data-driven procedure by which the final set of classifiers was selected gives insight into the sequence specificity of individual members within kinase families. This analysis reveals that, given the current data, it is often impossible to derive individual kinase-specific classifiers,

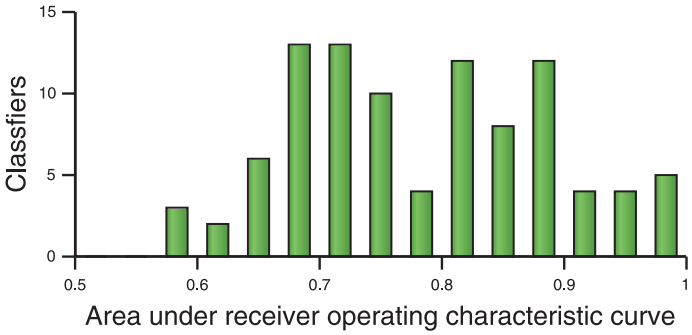

Fig. 3. Overview of the performance of the NetPhorest classifiers. The histogram shows the distribution of areas under the receiver operating characteristic curves (AROCs). More than 60% of the classifiers have AROC > 0.75 (see table S1 for the complete list of AROCs and fig. S8 or http://netphorest.info for the collection of ROCs).

even when sufficient data are available for several family members. In particular, it is clear that kinases of the Src family recognize the same, weak consensus sequence. In other words, the current data strongly suggest that these kinases are very similar at the motif level, implying that either they are functionally redundant or their specificity must be determined by the context in which the kinase is presented to a potential substrate. We recently showed that combining sequence motifs and contextual information greatly improves the accuracy with which kinases and substrates can be linked (*12*). This approach, NetworKIN, will benefit from the extended library of sequence motifs in NetPhorest.

The specificity of many kinases is provided in part through the recognition of binding motifs other than those containing the phosphorylation site itself; as an example, MAPKs typically bind short docking motifs within their substrates (*12*, *39*). Because all Src family kinases contain SH2 domains, which may help direct the kinases to their proper substrates, we tested if the tyrosine kinase domains that are linked to SH2 domains have lower sequence specificities than other tyrosine kinases and are reliant on an SH2 domain to function similar to a MAPK docking motif. Comparison of the predictive power (AROC) of the sequence models for the two groups of kinases revealed that this is indeed the case ($P < 10^{-3}$, Student's t test; Fig. 5A). We thus speculate that the combination of low-specificity kinase domains with interaction domains (for example, SH2 and SH3) and docking motifs, which provide specificity in a combinatorial fashion, is a common theme in phosphorylation-dependent signaling.

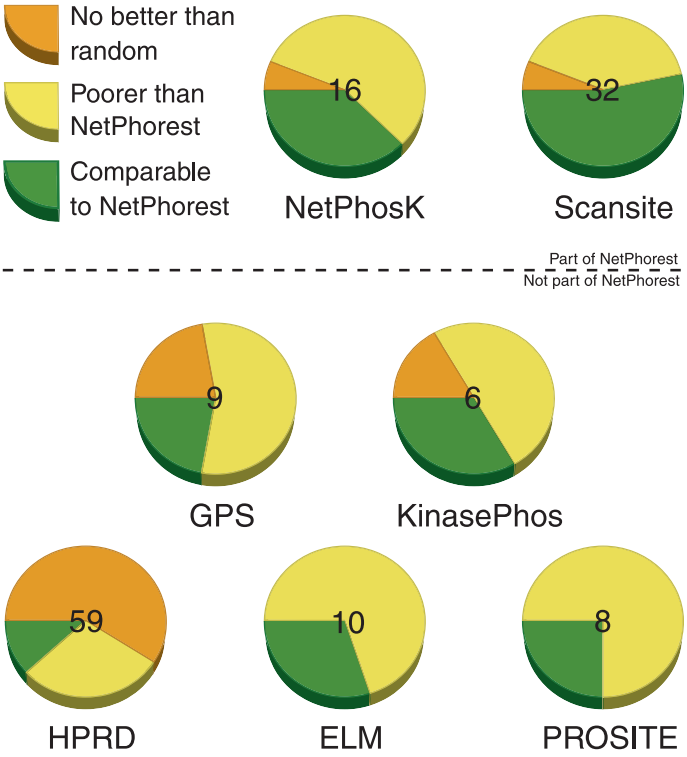

Fig. 4. Comparison of NetPhorest to other motif resources. We compared NetPhorest to Scansite (*13*) and the sequence patterns of ELM (*14*), PROSITE (*19*), and HPRD (*18*) using the entire compilation of phosphorylation sites. For NetPhosK (*20*), GPS (*22*), and KinasePhos (*24*), we used only the subset of sites that was dissimilar in sequence to those used to train classifiers of NetPhorest (see Methods for details). When at least five positive examples were left, the AROC was calculated. Subsequently, we tested how many of the predictors from each method performed no better than random, better than random but significantly poorer than NetPhorest, or comparable to NetPhorest. No predictor from any of the tested methods performed significantly better than the corresponding NetPhorest classifier. The number on each pie chart specifies how many predictors were tested from the method in question (see table S2 for details). Because classifiers from NetPhosK and Scansite were included in NetPhorest, those two resources are shown above the dotted line.

We further speculated that misregulation of kinases with low sequence specificity could induce particularly large changes in phosphorylation networks, which may lead to disease. This is supported by the observation that tyrosine kinases exhibit lower sequence specificity (AROC) than serine/threonine kinases ($P < 10^{-10}$, Student's t test; Fig. 5A) and are 10-fold more likely to harbor mutations that are causally implicated in cancer according to the Cancer Genome Project ($P < 10^{-8}$, Fisher's exact test). Furthermore, cancer-related tyrosine kinases, including those encoded by the *BCR–ABL* and *TEL–PDGFR* fusion oncogenes, have lower AROC than other tyrosine kinases ($P < 0.003$, Student's t test; Fig. 5B). Together these observations suggest that the global regulatory network changes observed in complex diseases, such as cancers, are in part due to nonspecific kinases, which potentially phosphorylate new substrates if they are abnormally expressed or become constitutively active.

Kinase activity is commonly regulated by autophosphorylation. It has been suggested (*40*, *41*) that the autophosphorylation sites of serine/threonine kinases differ in sequence from sites within other substrates. The motif scores for autophosphorylated sites in 10 serine/threonine kinases were significantly lower than those for other substrates of the same kinases ($P < 0.04$, Kolmogorov–Smirnov test; Fig. 5C). Our results thus support a structural study of three serine/threonine kinases (*41*) and suggest that weak sequence motifs may be a general feature of autophosphorylation sites.

In summary, we have presented a framework, NetPhorest, which automates the data set construction and training of sequence models for linear motifs. The framework was applied to current data for substrates of protein kinases and phosphorylation-dependent binding domains. The resulting classifiers have higher classification and predictive performance than existing methods and cover 179 kinases, 93 SH2 domains, 8 PTB domains as well as BRCT domains, WW domains, and 14-3-3 proteins. With technologies such as peptide arrays (*13*, *16*, *17*, *42*), phage display (*43*), and semisynthetic epitope construction (*44*), a rapid increase in the amount of linear motif data can be expected, stressing the importance of having a fully automated system for training, benchmarking, and selection of sequence models. Thus, as additional data become available for kinase docking motifs, phosphatases, or other types of modifications, these can readily be included in the atlas to provide a more complete picture of signaling networks.

We envisage that the NetPhorest atlas will be useful for many different aspects of signaling- and proteomics-related research (Fig. 6). First, there has been a recent trend in generating antibodies that recognize specific phosphorylated residues or sequences (phospho-specific antibodies). In particular, kinase "consensus motif antibodies," such as pS/T-Q, are powerful tools for both targeted studies (*12*) as well as systems studies (*45*). The atlas could be used to derive peptide sequences for raising such antibodies. A related use is for designing synthetic peptides that can be used to rewire cellular interaction networks or design new logic gates (*46*). In addition, mass spectrometry–based proteomics experiments frequently use simple sequence patterns for finding systematic biases in phosphopeptides identified in shotgun approaches (*8–11*). Such studies will benefit from the more robust and comprehensive collection of motifs in NetPhorest. Computational biology studies can, for example, use NetPhorest

for evolutionary studies of cellular signaling networks. Finally, NetPhorest will be used in future versions of the widely used resources Scansite (*13*), NetPhosK (*20*), and NetworKIN (*12*). Its ability to continuously incorporate the latest data will help accelerate systems-level modeling of cellular signaling events. Furthermore, we wish to develop NetPhorest into a global linear motif atlas by including other eukaryotic model organisms, such as yeast, as well as other types of posttranslational modifications. We cordially invite the scientific community to help expand the coverage of this resource by submitting data and purified active enzymes to the authors. The NetPhorest resource is released under the Creative Commons Attribution licenses and can be accessed at http://netphorest.info.

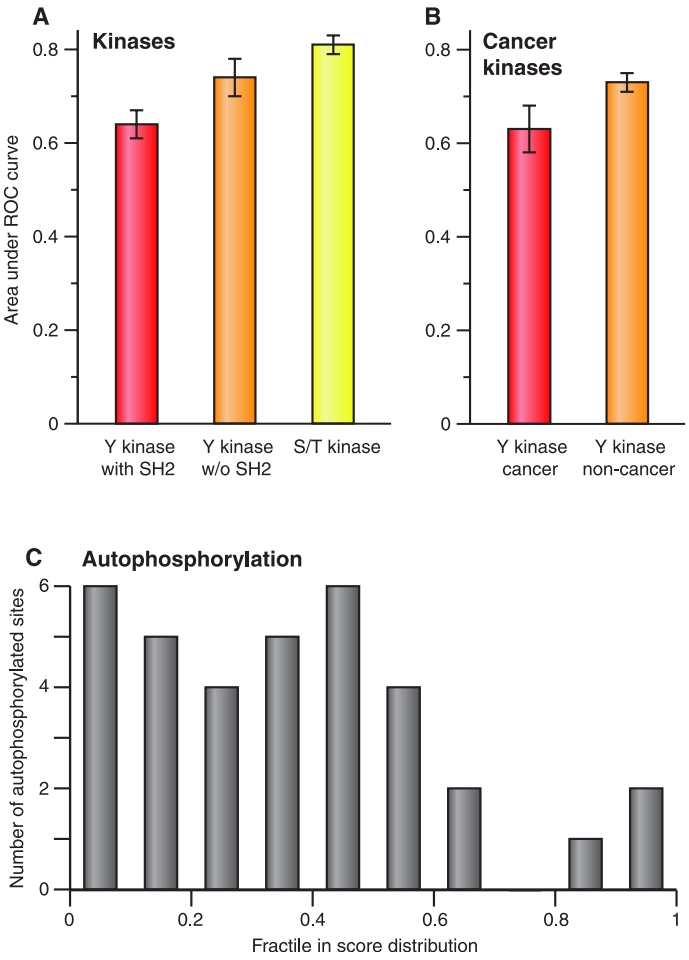

Fig. 5. Weak sequence specificity of oncogenic kinases and autophosphorylated sites. Using the AROC as a proxy for the degree of sequence specificity, we compared several subsets of kinases and SH2 domains. (**A**) Serine/threonine (S/T) kinases exhibit stronger sequence specificity (higher AROC) than tyrosine (Y) kinases ($P < 10^{-10}$). Tyrosine kinases with SH2 domains are less specific (lower AROC) than other tyrosine kinases ($P < 10^{-3}$). (**B**) Oncogenic tyrosine kinases, as defined by the Cancer Genome Project (*56*), have lower AROC than their non-oncogenic counterparts ($P < 0.003$). Error bars show the 90% confidence intervals and statistical significance was tested by Student's *t* test. (**C**) The score distribution of serine/threonine autophosphorylation sites in 10 kinases is shifted toward low values, whereas the random expectation would be a uniform distribution ($P < 0.04$; see Methods). This shows that autophosphorylation sites typically have weaker sequence motifs than other sites phosphorylated by the same kinase.

METHODS

Collection of published phosphorylation sites

To build ANN-based predictors and evaluate PSSMs for substrate recognition by kinases and phospho-binding domains, we collected phosphorylation data from several sources. The Phospho.ELM database (*26*) is the key repository for phosphorylation sites and contains more than 13,000 experimentally mapped phosphorylation sites of which most have been identified in vivo in mammalian proteins. An updated and hand-curated data set of 4169 experimentally verified kinase-specific phosphorylation sites distributed over 272 different kinases was obtained from version 7.0 of the Phospho.ELM database (*26*). From the PepCyber database (*47*), we obtained 948, 174, and 7 phosphoserine and phosphothreonine peptides previously shown to bind to 14-3-3 proteins and to the WW and BRCT domains, respectively.

From Phospho.ELM (*26*), we also obtained a set of 238 phosphotyrosine sites known to bind 45 different SH2 and PTB domains. We extended this data set by curating data from in vitro assays (*28*, *48*, *49*). For Smith *et al*. (*49*), the intensity threshold for a phosphotyrosine binding site was set to five times the intensity of the nonphosphorylated peptides. Furthermore, only phosphotyrosine-binding PTB domains (the APPL, DOK, FRS, and SHC families) (*49*) were included in the analysis (fig. S3). This yielded a total of 969 phosphotyrosine sites annotated to bind 67 and 8 different SH2 and PTB domains, respectively.

SH2 sites from high-density peptide arrays

A total of 6200 peptides, 13 amino acids long and containing a phosphotyrosine in the central position, were arrayed in three identical replicas on a microscope slide. The printed slides were incubated with SH2 domains fused to glutathione *S*-transferase (GST) and, after washing, the bound domains were identified and quantified by incubation with fluorescently labeled antibodies against GST. After background subtraction and averaging over the three replicas, each experiment yielded 6200 data points describing the peptide recognition profile of 66 specific SH2 domains (*34*).

Kinase matrices from positional scanning peptide libraries

Protein kinase phosphorylation motifs for Clk2, Clk3, LKB1, Mst1, Mst4, S6K1, Tlk1, and TNIK were determined with arrayed positional scanning peptide libraries (PSPL) as previously described (*16*). Briefly, we used a series of biotinylated peptides in which each of nine positions surrounding a central phosphorylation site was systematically substituted with each of the 20 proteogenic amino acids. This set of peptides was subjected in parallel to radiolabel kinase assays followed by capture on streptavidin membranes. Membranes were washed and exposed to a phosphor storage screen (fig. S6). To generate PSSMs for use with NetPhorest, spot intensities from at least two independent peptide library screens were quantified with ImageQuant software. Background subtracted data were normalized by dividing each value by the average of all values in a given position.

SH2 matrices from oriented peptide array libraries

The starting oriented peptide library contained the sequence KX3-pY-X5D, where X denotes a mixture of 19 naturally occurring amino acids (except for cysteine). Sublibraries containing substitutions of each X by an amino acid were synthesized on soluble nitrocellulose membranes on an Auto-Spot ASP 222 Robot (Abimed, CA). After being dissolved in a trifluoric acetic acid cocktail, these sublibraries, $19 \times 8 = 152$ in total, were printed onto Brady labels, producing multiple copies of identical oriented peptide array

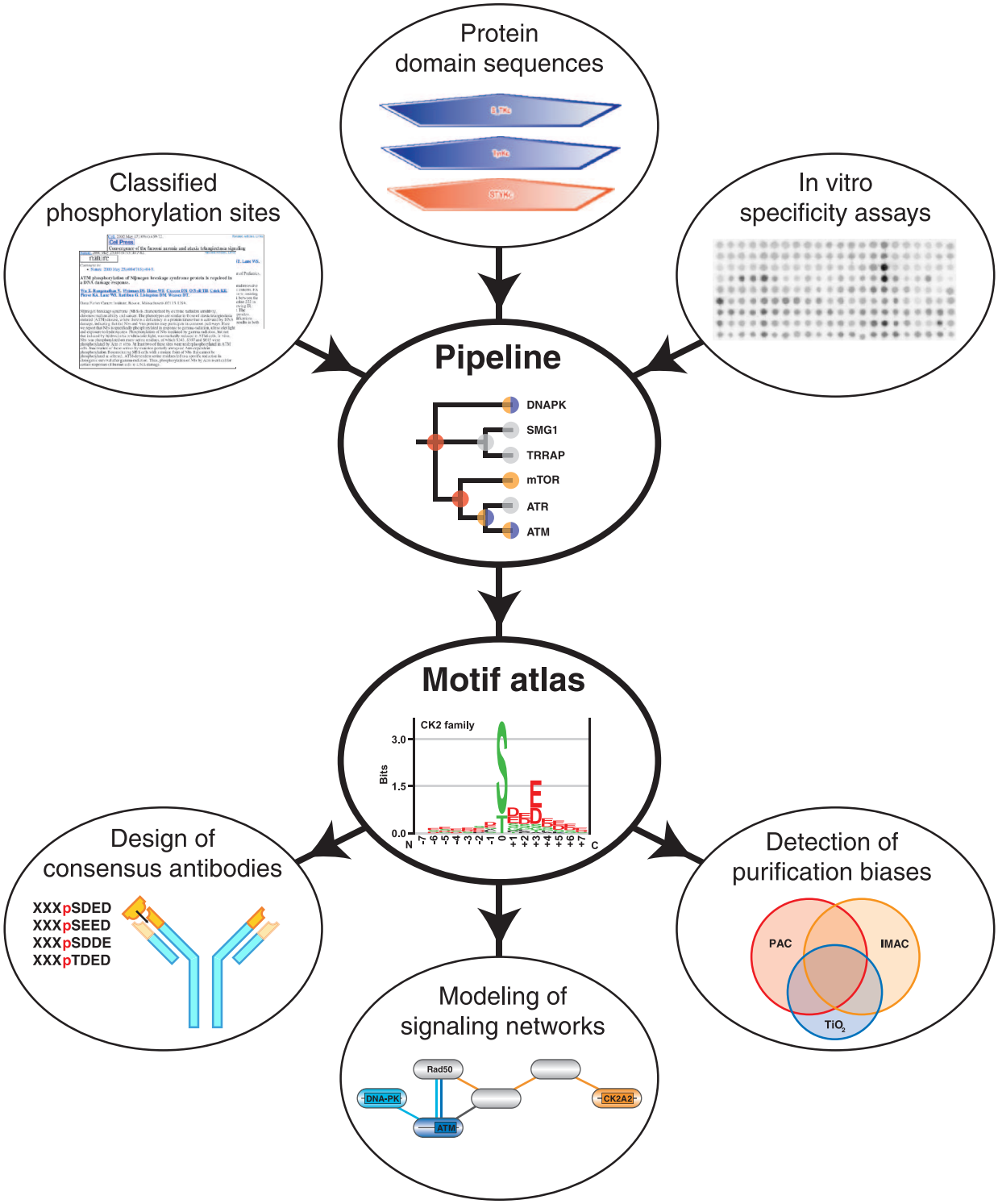

Fig. 6. The role of NetPhorest in phosphoproteomics and modeling of phosphorylation-dependent signaling networks. The NetPhorest atlas of consensus linear motifs can be used for designing synthetic peptides for the development of kinase- or family-specific antibodies (for example, pS/T-Q), will replace Scansite (*13*) and NetPhosK (*20*) as the motif component of the NetworKIN resource (http://networkin.info) (*12*, *57*), and can be used to detect biases arising from the enrichment procedures commonly used in phosphoproteomics [for example, phosphoramidate chemistry (PAC), immobilized metal affinity chromatography (IMAC), and titanium oxide (TiO_2) (*58*)]. The NetPhorest Web site (http://netphorest.info) provides the means to classify phosphorylation sites on the basis of consensus sequence motifs.

libraries (OPAL). Screening of an OPAL membrane with a purified GST–SH2 domain fusion protein yielded a defined binding pattern that was subsequently imaged and quantified. The above binding data were used to generate a matrix used in the prediction of SH2-binding peptides (*33*). To ensure high-quality PSSMs, only those with information content above 2 bits (not considering the central phosphorylated residue) were included. This threshold was estimated by manual inspection of the raw images.

Position-specific scoring matrices

For this work, we collected the most comprehensive set to date of PSSMs from previously published works, from unpublished data, and from experiments specifically made for this study. From the Scansite database (*13*), we obtained 20, 11, and 1 PSSMs for kinases and SH2 and PTB domains, respectively. Combined with the PSPL and OPAL data described above, this yields a collection of PSSMs that covers 50 kinases, 77 SH2 domains, and 1 PTB domain. Information on both positive and negative selection of residues at each position is used.

Construction of phylogenetic domain trees

To obtain a phylogenetic tree file of the human kinome, tree files for the individual kinase superfamilies were downloaded from http://kinase.com/human/kinome/phylogeny.html. These files were manually merged and edited to obtain a kinase tree consistent with the one published by Manning *et al*. (*25*). The SH2 domain tree file was manually constructed according to the dendogram of the human SH2 domains shown in (*29*). To produce the 14-3-3 and PTB domain trees, we extracted the sequences of these domains as predicted by SMART (*3*), aligned these with MAFFT (*50*), identified conserved blocks with Gblocks (*51*), and constructed a maximum likelihood tree with PhyML (*52*).

Tree-based data organization

To enable mapping of all experimentally determined phosphorylation sites and PSSMs onto the domain trees described above, we standardized the kinase and phospho-binding domain names used in each data source to follow the Phospho.ELM nomenclature (while maintaining a mapping to HGNC and KinBase names). Using the phylogenetic trees of kinase and phospho-binding domains as guides, we partitioned the data into specific (terminal nodes) or family-based (internal nodes) subsets. These subsets constituted the positive data for ANN training. The remaining part of the total data set was used as negative data, except if the data were assigned directly to upstream parental nodes.

For each specific or family-based predictor, the positive and negative data sets were pooled and redundancy reduced. This was first performed on full-length proteins and subsequently on 13-mer peptide level (positive or negative phosphorylation site centrally placed) by use of CD-HIT (*53*) with default values and 90% sequence identity threshold in both cases. The amino acids that were not annotated as phosphorylation sites in the positive data were pruned from the negative data. For example, because adenosine protein kinase A (PKA) phosphorylates serine and threonine and not tyrosine, the phosphotyrosine sites were removed from the negative data.

Artificial neural network training

In this work, we used a standard three-layer feed-forward network that was trained with the backpropagation algorithm as previously described (*54*). To balance the training, we reduced the negative data sets to only contain five negative examples per positive example. At least 12 positive sites after redundancy reduction were required before an ANN was trained. The resulting data set was divided into four subsets by random partitioning. We trained an ANN on two subsets, determined the optimal network architecture and training parameters on the third subset, and obtained an unbiased performance estimate from the fourth subset. This was repeated in a round-robin fashion to use all data for training, test, and validation. The following ANN parameters were varied to optimize Matthews correlation coefficient on each test set: the window size (5, 7, 9, 11, and 13 for phospho-binding domains and up to 21 for kinases), the number of hidden neurons (0, 2, 4, 6, 10, 15, and 20), and the learning rate (0.05, 0.01, and 0.005). The three best parameter combinations from each cross-validation were kept to obtain an ensemble of 12 ANNs. This improved the predictive performance compared to using only the best parameter combination, whereas using a larger ensemble did not lead to further improvement but made the method markedly slower. We calculated the AROC by applying each ANN to the corresponding independent validation set. For unclassified sites, we averaged the output of the ANNs in each ensemble. The training data and the classifiers are available at http://netphorest.info.

Score calibration

To make the output scores from different PSSMs comparable, we calculated a scaling factor for each PSSM on the basis of its score distribution on random peptides. We then calibrated the scores from both ANNs and PSSMs through benchmarking on the compilation of phosphorylation sites. The positive predictive value [true positives/(true positives + false positives)] was calculated within different score windows (running bins) on the validation set. Subsequently, we fitted a logistic function to these values, minimizing the sum of squared errors. We chose the logistic function on the basis of visual inspection of the calibration plots and because it is monotonic.

For about one-third of the PSSMs (47 of 142), a sigmoid function could not be estimated because not enough corresponding phosphorylation sites were available for benchmarking (less than 12 positive examples). Assuming that these PSSMs have comparable performances to those that could be evaluated, we calculated a general PSSM sigmoid on the basis of data from the PSSMs that we were able to benchmark. In this way, we calculated three general sigmoid curves for kinases, SH2 domains, and PTB domains, respectively.

Because the fraction of positive examples in the evaluation set does not reflect the prior probability of a site being phosphorylated by a particular family of kinases, the sigmoid curve does not directly yield the posterior probability. To correct for this, we assumed that the prior probability is $\sqrt{N}/50$ for kinases, $\sqrt{N}/35$ for phospho-binding domains, where N is the number of domains in the family in question. These values are largely arbitrary but correspond to guessing that, in vivo, each phosphorylation site can on average be phosphorylated by 10 different kinases and bound by 2 phospho-binding domains. It should be noted that the choice of these parameters have no influence on the performance of each classifier, and hence also not on which classifiers are selected by the procedure described below.

Sequence similarity of domains

Pairwise sequence similarity was calculated [with the ParAlign software (*55*)] as self-normalized bit scores between all domain sequences in the kinase, SH2, and PTB domain trees. The self-normalized bit scores of domains A and B were calculated as the bit score of A to B divided by the minimum of the bit score of A to A and B to B. For internal nodes in the trees, the pairwise sequence similarity was calculated as the average similarity of all members of the family to all members of the family in question.

Placement of PSSMs and ANNs in the trees

ANNs were trained for all possible nodes in the trees with the phosphorylation site data described above. The PSSMs used in this work were based

on in vitro experiments, which were always performed with a specific immunoprecipitated or otherwise purified domain. However, the resulting PSSM may be better used as a classifier for a family including other closely related domains. To investigate this, the phosphorylation site data set was used to benchmark each PSSM considering it as a classifier at every node on the path connecting the root of the tree with the node at which the PSSM was initially assigned. Using the pairwise domain sequence similarity described above, we eliminated families with a self-normalized bit score less than 0.3. This threshold was chosen on the basis of the fact that above a domain similarity score of 0.3, there is a significant correlation between domain sequence similarity and substrate similarity (fig. S5).

Selection of classifiers

The predictive performance of the ANN and PSSM classifiers was estimated by calculating the AROC with the compilation of phosphorylation sites. We discarded any classifiers not performing significantly better than random ($P < 0.05$), as judged from a bootstrapped AROC distribution constructed by resampling the scores of positive and negative examples. The PSSMs that could not be benchmarked were assumed to have comparable performance to other PSSMs obtained from the same type of assay, and were thus assigned the average AROC of the PSSMs that could be benchmarked. Any domains that were not covered by a given set of classifiers were considered equivalent to random performance (AROC = 0.5).

At each node in the tree, we selected the classifier with the highest AROC. If multiple PSSMs have identical AROC, the one with the highest Kullback–Leibler information content was chosen. To obtain a nonredundant set of classifiers, the average AROC was maximized across all domains with a recursive procedure that starts from the leaf nodes. When multiple solutions had identical AROC, we chose the one that covered the largest number of domains.

Benchmarking of published methods

To perform a fair benchmark of the available methods for predicting kinase-specific phosphorylation, we constructed a validation set consisting of phosphorylation sites that were not used during training of the respective methods. To this end we obtained the training data sets from the authors of GPS (*22*) and KinasePhos (*24*) and removed identical or highly similar phosphoproteins from our compilation of phosphorylation sites with the same criteria as for redundancy reduction. The resulting independent validation sets consisted of 182 and 79 phosphorylation sites for GPS and KinasePhos, respectively. We applied each prediction method to its respective validation set and calculated the AROC for the kinases or family of kinases for which we had at least five phosphorylation sites in the validation set. To test if the observed performance was significantly higher than random or significantly poorer than NetPhorest, we constructed bootstrap estimates of the uncertainty associated with each AROC by resampling of the score distributions for positive and negative examples.

We used a similar procedure for benchmarking the sequence patterns (for example, [ST]P.[RK])from ELM (*14*), PROSITE (*19*), and HPRD (*18*). As multiple regular expressions may be provided for the same domain or family of domains, we scored each site on the basis of the fraction of the sequence patterns that matched the site. As we have no way of determining which sites were used for deriving the regular expressions, the complete, nonredundant compilation of phosphorylation sites was used for benchmarking them.

Analysis of substrate specificity for oncogenic kinases

A complete list of genes for which mutations (both germline and somatic) have been causally implicated in cancer was obtained from the Cancer Genome Project (Cancer Gene Census catalog version 2007.02.13, http://www.sanger.ac.uk/genetics/CGP/) (*56*). The list was matched to the set of serine/threonine and tyrosine kinases in the NetPhorest atlas. The fraction of protooncogenes in each set was calculated and compared by Fisher's exact test. Subsequently, the average AROC was calculated for oncogenic and non-oncogenic tyrosine kinases compared by Student's *t* test.

Comparison of autophosphorylated sites and other phosphorylation sites

We extracted all autophosphorylated sites in the Phospho.ELM database (*26*) and scored them with NetPhorest. The resulting posterior probabilities were converted to fractiles in the score distribution of all known phosphorylation sites for the kinase in question. The distribution of fractiles was compared to random expectation (uniform distribution) by the Kolmogorov–Smirnov test.

SUPPLEMENTARY MATERIALS

www.sciencesignaling.org/cgi/content/full/1/35/ra2/DC1
Figure S1: Overview of the NetPhorest pipeline.
Figure S2: Phosphorylation data mapped onto domain trees.
Figure S3: Coverage of classifiers for targets of kinases, SH2 domains, and PTB domains.
Figure S4: Score calibration.
Figure S5: Correlation between domain similarity and substrate specificity.
Figure S6: Kinase matrices from Positional Scanning Peptide Libraries (PSPL).
Figure S7: Sequence logos for kinases and pS/pT-binding domains.
Figure S8: Receiver output characteristic (ROC) curves for the NetPhorest classifiers.
Table S1: The selected set of NetPhorest classifiers.
Table S2: Benchmark of the NetPhorest method.
Poster: A Sequence-Specificity Atlas of the Kinase World

REFERENCES AND NOTES

1. R. Linding, R. B. Russell, V. Neduva, T. J. Gibson, GlobPlot: Exploring protein sequences for globularity and disorder. *Nucleic Acids Res.* **31**, 3701–3708 (2003).
2. R. D. Finn, J. Mistry, B. Schuster-Böckler, S. Griffiths-Jones, V. Hollich, T. Lassmann, S. Moxon, M. Marshall, A. Khanna, R. Durbin, S. R. Eddy, E. L. Sonnhammer, A. Bateman, Pfam: Clans, web tools and services. *Nucleic Acids Res.* **34**, D247–D251 (2006).
3. I. Letunic, R. R. Copley, B. Pils, S. Pinkert, J. Schultz, P. Bork, SMART 5: Domains in the context of genomes and networks. *Nucleic Acids Res.* **34**, D257–D260 (2006).
4. M. B. Yaffe, "Bits" and pieces. *Sci. STKE* **2006**, pe28 (2006).
5. L. J. Jensen, T. S. Jensen, U. de Lichtenberg, S. Brunak, P. Bork, Co-evolution of transcriptional and posttranslational cell-cycle regulation. *Nature* **443**, 594–597 (2006).
6. V. Neduva, R. B. Russell, Linear motifs: Evolutionary interaction switches. *FEBS Lett.* **579**, 3342–3345 (2005).
7. C. Jørgensen, R. Linding, Directional and quantitative phosphorylation networks. *Brief Funct Genomic Proteomic.* **7**, 17–26 (2008).
8. S. A. Beausoleil, M. Jedrychowski, D. Schwartz, J. E. Elias, J. Villen, J. Li, M. A. Cohn, L. C. Cantley, S. P. Gygi, Large-scale characterization of HeLa cell nuclear phosphoproteins. *Proc. Natl. Acad. Sci. U.S.A.* **101**, 12130–12135 (2004).
9. J. V. Olsen, B. Blagoev, F. Gnad, B. Macek, C. Kumar, P. Mortensen, M. Mann, Global, in vivo, and site-specific phosphorylation dynamics in signaling networks. *Cell.* **127**, 635–648 (2006).
10. J. Malmström, H. Lee, R. Aebersold, Advances in proteomic workflows for systems biology. *Curr. Opin Biotechnol.* **18**, 378–384 (2007).
11. A. Wolf-Yadlin, S. Hautaniemi, D. A. Lauffenburger, F. M. White, Multiple reaction monitoring for robust quantitative proteomic analysis of cellular signaling networks. *Proc. Natl. Acad. Sci. U.S.A.* **104**, 5860–5865 (2007).
12. R. Linding, L. J. Jensen, G. J. Ostheimer, M. A. van Vugt, C. Jørgensen, I. M. Miron, F. Diella, K. Colwill, L. Taylor, K. Elder, P. Metalnikov, V. Nguyen, A. Pasculescu, J. Jin, J. G. Park, L. D. Samson, J. R. Woodgett, R. B. Russell, P. Bork, M. B. Yaffe, T. Pawson, Systematic discovery of in vivo phosphorylation networks. *Cell* **129**, 1415–1426 (2007).
13. J. C. Obenauer, L. C. Cantley, M. B. Yaffe, Scansite 2.0: Proteome-wide prediction of cell signaling interactions using short sequence motifs. *Nucleic Acids Res.* **31**, 3635–3641 (2003).
14. P. Puntervoll, R. Linding, C. Gemund, S. Chabanis-Davidson, M. Mattingsdal, S. Cameron, D. M. Martin, G. Ausiello, B. Brannetti, A. Costantini, F. Ferre, V. Maselli, A. Via, G. Cesareni, F. Diella, G. Superti-Furga, L. Wyrwicz, C. Ramu, C. McGuigan, R. Gudavalli, I. Letunic, P. Bork, L. Rychlewski, B. Kuster, M. Helmer-Citterich, W. N. Hunter, R. Aasland, T. J. Gibson, ELM server: A new resource for investigating short functional sites in modular eukaryotic proteins. *Nucleic Acids Res.* **31**, 3625–3630 (2003).

15. T. Obata, M. B. Yaffe, G. G. Leparc, E. T. Piro, H. Maegawa, A. Kashiwagi, R. Kikkawa, L. C. Cantley, Peptide and protein library screening defines optimal substrate motifs for AKT/PKB. *J. Biol. Chem.* **275**, 36108–16115 (2000).
16. J. E. Hutti, E. T. Rarrell, J. D. Chang, D. W. Abbott, P. Storz, A. Toker, L. C. Cantley, B. E. Turk, A rapid method for determining protein kinase phosphorylation specificity. *Nat. Methods* **1**, 27–29 (2004).
17. M. Rodriguez, S. S.-C. Li, J. W. Harper, Z. Songyang, An oriented peptide array library (OPAL) strategy to study protein-protein interactions. *J. Biol. Chem.* **279**, 8802–8807 (2004).
18. R. Amanchy, B. Periaswamy, S. Mathivanan, R. Reddy, S. G. Tattikota, A. Pandey, A curated compendium of phosphorylation motifs. *Nat. Biotechnol.* **25**, 285–286 (2007).
19. N. Hulo, A. Bairoch, V. Bulliard, L. Cerutti, B. A. Cuche, E. De Castro, C. Lachaize, P. S. Langendijk-Genevaux, C. J. A. Sigrist, The 20 years of PROSITE. *Nucleic Acids Res.* **36**, D245–D249 (2008).
20. N. Blom, T. Sicheritz-Pontén, R. Gupta, S. Gammeltoft, S. Brunak, Prediction of post-translational glycosylation and phosphorylation of proteins from the amino acid sequence. *Proteomics* **4**, 1633–1649 (2004).
21. J. H. Kim, J. Lee, B. Oh, K. Kimm, I. Koh, Prediction of phosphorylation sites using SVMs. *Bioinformatics* **20**, 3179–3184 (2004).
22. Y. Xue, F. Zhou, M. Zhu, K. Ahmed, G. Chen, X. Yao, GPS: A comprehensive www server for phosphorylation sites prediction. *Nucleic Acids Res.* **33**, W184–W187 (2005).
23. Y. Xue, A. Li, L. Wang, H. Feng, X. Yao, PPSP: Prediction of PK-specific phosphorylation site with Bayesian decision theory. *BMC Bioinformatics* **7**, 163 (2006).
24. Y. H. Wong, T. Y. Lee, H. K. Liang, C. M. Huang, T. Y. Wang, Y. H. Yang, C. H. Chu, H. D. Huang, M. T. Ko, J. K. Hwang, KinasePhos 2.0: A web server for identifying protein kinase-specific phosphorylation sites based on sequences and coupling patterns. *Nucleic Acids Res.* **35**, W588–W594 (2007).
25. G. Manning, D. B. Whyte, R. Martinez, T. Hunter, S. Sudarsanam, The protein kinase complement of the human genome. *Science* **298**, 1912–1934 (2002).
26. F. Diella, C. M. Gould, C. Chica, A. Via, T. J. Gibson, Phospho.ELM: A database of phosphorylation sites—update 2008. *Nucleic Acids Res.* **36**, D240–D244 (2008).
27. A. Ceol, A. Chatr-aryamontri, E. Santonico, R. Sacco, L. Castanogli, G. Cesareni, DOMINO: A database of domain-peptide interactions. *Nucleic Acids Res.* **35**, D557–D560 (2007).
28. R. B. Jones, A. Gordus, J. A. Krall, G. MacBeath, A quantitative protein interaction network for the ErbB receptors using protein microarrays. *Nature* **439**, 168–174 (2006).
29. B. A. Liu, K. Jablonowski, M. Raina, M. Arcé, T. Pawson, P. D. Nash, The human and mouse complement of SH2 domain proteins—establishing the boundaries of phosphotyrosine signaling. *Mol. Cell* **22**, 851–868 (2006).
30. P. Baldi, S. Brunak, Y. Chauvin, C. A. F. Andersen, H. Nielsen, Assessing the accuracy of prediction algorithms for classification: An overview. *Bioinformatics* **16**, 412–424 (2000).
31. I. A. Manke, A. Nguyen, D. Lim, M. Q. Stewart, A. E. Elia, M. B. Yaffe, MAPKAP kinase-2 is a cell cycle checkpoint kinase that regulates the G2/M transition and S phase progression in response to UV irradiation. *Mol. Cell* **17**, 37–48 (2005).
32. A. Krogh, What are artificial neural networks? *Nat. Biotechnol.* **26**, 195–197 (2008).
33. H. Huang, L. Li, C. Wu, D. Schibli, K. Colwill, S. Ma, C. Li, P. Roy, K. Ho, Z. Songyang, T. Pawson, Y. Gao, S. S. Li, Defining the specificity space of the human SRC homology 2 domain. *Mol. Cell. Proteomics.* **7**, 768–784 (2008).
34. The data are available from the NetPhorest Web site (http://netphorest.info).
35. J. E. Hansen, O. Lund, N. Tolstrup, A. A. Gooley, K. L. Williams, S. Brunak, NetOglyc: Prediction of mucin type O-glycosylation sites based on sequence context and surface accessibility. *Glycoconj. J.* **15**, 115–130 (1998).
36. H. Nielsen, S. Brunak, G. von Heijne, Machine learning approaches for the prediction of signal peptides and other protein sorting signals. *Protein Eng.* **12**, 3–9 (1999).
37. L. J. Jensen, R. Gupta, H.-H. Stærfeldt, S. Brunak, Prediction of human protein function according to Gene Ontology categories. *Bioinformatics* **19**, 635–642 (2003).
38. J. A. Hanley, B. J. McNeil, The meaning and use of the area under a receiver operating characteristic (ROC) curve. *Radiology* **143**, 29–36 (1982).
39. A. Ubersax, J. Ferrell, Jr., Mechanisms of specificity in protein phosphorylation. *Nat. Rev. Mol. Cell. Biol.* **8**, 530–541 (2007).
40. A. W. Oliver, S. Knapp, L. H. Pearl, Activation segment exchange: A common mechanism of kinase autophosphorylation? *Trends Biochem. Sci.* **32**, 351–356 (2007).
41. A. C. W. Pike, P. Rellos, F. H. Niesen, A. Turnbull, A. W. Oliver, S. A. Parker, B. E. Turk, L. H. Pearl, S. Knapp, Dimerization by activation segment exchange reveals a mechanism for kinase auto-phosphorylation. *EMBO J.* **27**, 704–714 (2008).
42. C. Landgraf, S. Panni, L. Montecchi-Palazzi, L. Castanogli, J. Schneider-Mergener, R. Volkmer-Engert, G. Cesareni, Protein interaction networks by proteome peptide scanning. *PLoS Biol.* **2**, 94–103 (2004).
43. S. S. Sidhu, S. Koide, Phage display for engineering and analyzing protein interaction interfaces. *Curr. Opin. Struct. Biol.* **17**, 481–487 (2007).
44. J. J. Allen, M. Li, C. S. Brinkworth, J. L. Paulson, D. Wang, A. Hübner, W.-H. Chou, R. J. Davis, A. L. Burlingame, R. O. Messing, C. D. Katayama, S. M. Hedrick, K. M. Shokat, A semisynthetic epitope for kinase substrates. *Nat. Methods* **4**, 511–516 (2007).
45. S. Matsuoka, B. A. Ballif, A. Smogorzewska, E. R. McDonald III, K. E. Hurov, J. Luo, C. E. Bakalarski, Z. Zhao, N. Solimini, Y. Lerenthal, Y. Shiloh, S. P. Gygi, S. J. Elledge, ATM and ATR substrate analysis reveals extensive protein networks responsive to DNA damage. *Science* **316**, 1160–1166 (2007).
46. J. E. Dueber, E. A. Mirsky, W. A. Lim, Engineering synthetic signaling proteins with ultrasensitive input/output control. *Net. Biotechnol.* **25**, 660–662 (2007).
47. W. Gong, D. Zhou, Y. Ren, Y. Wang, Z. Zuo, Y. Shen, F. Xiao, Q. Zhu, A. Hong, X. Zhou, X. Gao, T. Li, Pepcyber:P~PEP: A database of human protein protein interactions mediated by phosphoprotein-binding domains. *Nucleic Acids Res.* **36**, D679–D683 (2008).
48. W. X. Schulze, L. Deng, M. Mann, Phosphotyrosine interactome of the ErbB-receptor kinase family. *Mol. Syst. Biol.* **1**, 2005.0008 (2005).
49. M. J. Smith, W. R. Hardy, J. M. Murphy, N. Jones, T. Pawson, Screening for PTB domain binding partners and ligand specificity using proteome-derived NPXY peptide arrays. *Mol. Cell. Biol.* **26**, 8461–8474 (2006).
50. K. Katoh, K. Kuma, H. Toh, T. Miyata, MAFFT version 5: Improvement in accuracy of multiple sequence alignment. *Nucleic Acids Res.* **33**, 511–518 (2005).
51. G. Talavera, J. Castresana, Improvement of phylogenies after removing divergent and ambiguously aligned blocks from protein sequence alignments. *Syst. Biol.* **56**, 564–577 (2007).
52. S. Guindon, O. Gascuel, A simple, fast, and accurate algorithm to estimate large phylogenies by maximum likelihood. *Syst. Biol.* **52**, 696–704 (2003).
53. W. Li, A. Godzik, Cd-hit: A fast program for clustering and comparing large sets of protein or nucleotide sequences. *Bioinformatics* **22**, 1658–1659 (2006).
54. N. Blom, S. Gammeltoft, S. Brunak, Sequence and structure-based prediction of eukaryotic protein phosphorylation sites. *J. Mol. Biol.* **294**, 1351–1362 (1999).
55. T. Rognes, E. Seeberg, Six-fold speed-up of Smith–Waterman sequence database searches using parallel processing on common microprocessors. *Bioinformatics* **16**, 699–706 (2000).
56. P. A. Futreal, L. Coin, M. Marshall, T. Down, T. Hubbard, R. Wooster, N. Rahman, M. R. Stratton, A census of human cancer genes. *Nat. Rev. Cancer.* **4**, 177–183 (2004).
57. R. Linding, L. J. Jensen, A. Pasculescu, M. Olhovsky, K. Colwill, P. Bork, M. B. Yaffe, T. Pawson, NetworKIN: A resource for exploring cellular phosphorylation networks. *Nucleic Acids Res.* **36**, D695–D699 (2008).
58. B. Bodenmiller, L. N. Mueller, M. Mueller, B. Domon, R. Aebersold, Reproducible isolation of distinct, overlapping segments of the phosphoproteome. *Nat Methods* **4**, 231–237 (2007).

59. Thanks to S. Quirk and K. Colwill (Samuel Lunenfeld Research Institute) for commenting on the manuscript. We thank T. N. Petersen, S. Gammeltoft, and M. Hjerrild for discussions, P. Nash for help in generating the SH2 tree, and I. Letunic (European Molecular Biology Laboratory), K. Colwill (Samuel Lunenfeld Research Institute), C. Workman, and A. G. Pedersen (Center for Biological Sequence Analysis) for technical help and assistance. We thank the Protein Modules Consortium (www.proteinmodules.org) for encouraging the project, and the authors of GPS, KinasePhos, and NetPhosK who kindly shared their training data, enabling us to benchmark these methods. We thank N. Warner (U of T) for sharing peptide data prior to publication. We thank R. J. Shaw (Salk Institute) and T. J. McGarry (Northwestern University) for LKB1 and TLK1 kinase, respectively. R.L. was supported by a Human Frontiers Science Programme fellowship. This project was supported by The Institute of Cancer Research (ICR), The Lundbeck Foundation, The Novo Nordisk Foundation, Genome Canada through Ontario Genomics Institute, National Cancer Institute of Canada, the NIH (U54-CA112967 and R01 GM60594), and by Interaction Proteome (contract number LSHG-CT-2003-505520), the BioSapiens Network of Excellence (contract number LSHG-CT-2003-503265), the EMBRACE network of excellence (contract number LHSG-CT-2004-512092), the ENFIN network of excellence (contract number LSHG-CT-2005-518254), the ADIT Integrated Project (contract number LSHB-CT-2005-511977), and the GeneFun Specific Targeted Research Project (contract numbers LSHG-CT-2004-503567 and LSHB-CT-2004-512143), all six funded by the European Commission FP6 Programme. The Structural Genomics Consortium is a registered charity (number 1097737) that receives funds from the Canadian Institutes for Health Research, the Canadian Foundation for Innovation, GlaxoSmithKline, Karolinska Institutet, the Knut and Alice Wallenberg Foundation, the Ontario Innovation Trust, the Ontario Ministry for Research and Innovation, Merck & Co., Inc., the Novartis Research Foundation, the Swedish Agency for Innovation Systems, the Swedish Foundation for Strategic Research, and the Wellcome Trust.

Submitted 21 April 2008
Accepted 24 July 2008
Final Publication 2 September 2008
10.1126/scisignal.1159433

Citation: M. L. Miller, L. J. Jensen, F. Diella, C. Jørgensen, M. Tinti, L. Li, M. Hsiung, S. A. Parker, J. Bordeaux, T. Sicheritz-Ponten, M. Olhovsky, A. Pasculescu, J. Alexander, S. Knapp, N. Blom, P. Bork, S. Li, G. Cesareni, T. Pawson, B. E. Turk, M. B. Yaffe, S. Brunak, R. Linding, Linear motif atlas for phosphorylation-dependent signaling. *Sci. Signal.* **1**, ra2 (2008).